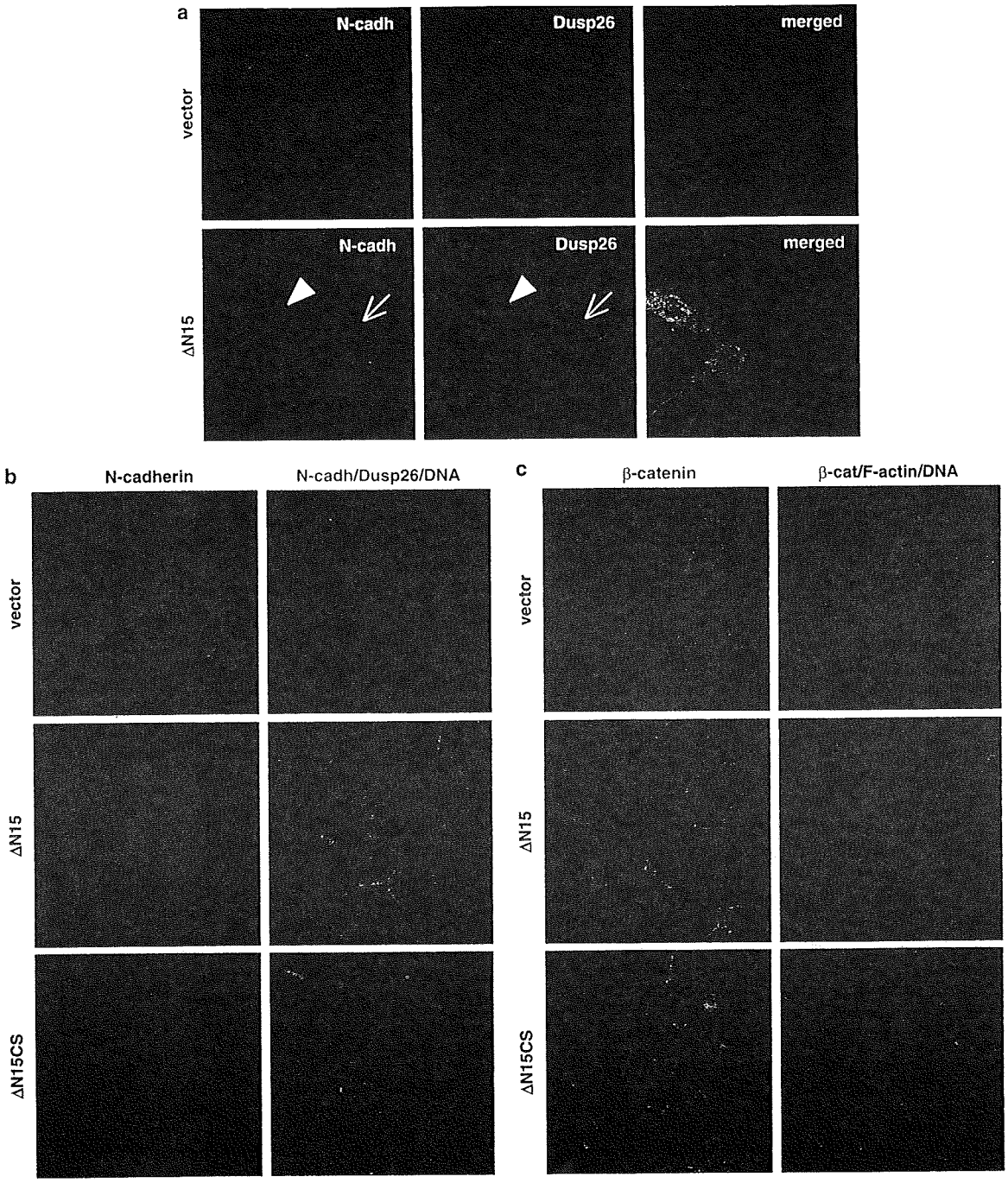


**Figure 6** Enhanced N-cadherin and β-catenin localization at cell–cell contact sites of cells expressing Dusp26. **(a)** Representative images of immunostaining of NIH3T3 cells infected with Dusp26 or vector alone. Cells on coverslips coated with collagen and seeded at low density were immunostained with anti-N-cadherin (N-cadh) and anti-Dusp26 (Dusp26) antibodies. Shown are single sections obtained by confocal scans. Note Dusp26 and N-cadherin colocalization at the membrane ruffle (indicated by arrows) but not at cell–cell contact sites (arrowhead), where N-cadherin is also enriched. **(b, c)** Enhanced N-cadherin (b) and β-catenin (c) localization at cell–cell contact sites mediated by Dusp26. Cells were seeded at higher densities to allow contact and analysed for N-cadherin (N-cadh) and Dusp26 (b), and for β-catenin (β-cat) and F-actin (c). DRAQ5 staining shows similar cell densities of the fields.

tissue architecture. Altered adhesiveness is often associated with increased cell motility, invasiveness and tumor metastasis. We have shown that Dusp26 dephosphorylates the Kap3 subunit of the KIF3 motor and promotes localization of N-cadherin/β-catenin to sites of cell–cell contact, resulting in enhanced adhesion.

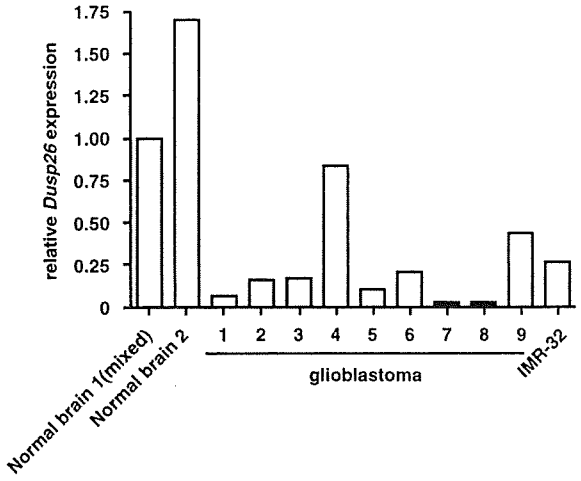


**Figure 7** Analysis of Dusp26 mRNA levels in primary tumor samples. Downregulation of Dusp26 mRNA in primary glioblastoma samples and a neuroblastoma cell line. Expression levels of Dusp26 mRNA in human primary glioblastoma samples were estimated by qRT-PCR. Results were normalized to mRNA levels of the housekeeping gene porphobilinogen deaminase (*PBGD*) and shown as relative to mRNA levels seen in normal brain (normal brains (mixed)), which was set as 1.0. Also shown is Dusp26 expression in the human IMR-32 neuroblastoma cell line.

It has been established that post-Golgi transport of β-catenin/Cadherin(s) to the plasma membrane is mediated by the KIF3 motor (Jimbo *et al.*, 2002; Teng *et al.*, 2005). Although the detailed mechanisms by which Dusp26 enhances distribution of N-cadherin/β-catenin remain unclear, they likely involve Kap3 dephosphorylation by Dusp26, since expression of its inactive mutant does not alter $Ca^{2+}$-dependent adhesion (Figure 5) or N-cadherin localization (data not shown). Accumulated evidence reveals the importance of molecular motors such as myosin, dynein and KIF proteins in organelle transport, but it remains largely unknown how binding and release of cargo at destination sites are regulated. Our results suggest a possible function for Kap3 phosphorylation in these processes. Previous studies in which phosphorylation of the myosin-V and KIF17 motors by calcium/calmodulin-dependent protein kinase II were suggested to control docking of cargo (Karcher *et al.*, 2001; Guillaud *et al.*, 2008) support our hypothesis. Identification of Kap3 phosphorylation site(s) is the next critical step to address these issues.

Analysis of human glioblastoma revealed that *Dusp26* expression was low compared to that seen in normal brain in most samples. Given that cell–cell adhesion was enhanced in cells expressing Dusp26, these results suggest tumor-suppressing activities of Dusp26, and that *Dusp26* gene is silenced and/or deactivated in glioma. Dusp26 downregulation may be associated with invasive phenotypes of glioblastomas, although mechanisms underlying Dusp26 downregulation are not known.

In summary, Dusp26 dephosphorylates Kap3, enhances cell–cell adhesion by promoting localization of N-cadherin/β-catenin at sites of cell–cell contact and is downregulated in human glioblastomas. Further investigation to elucidate mechanisms regulating Dusp26 expression in brain tumors and identify kinase(s) responsible for Kap3 phosphorylation is required to understand how dysregulation of intracellular transport and cell–cell adhesion coincides with tumor development.

## Materials and methods

*Antibodies*

Anti-Flag M2 and anti-Myc 9E10 antibody were purchased from Sigma (St Louis, MO, USA) and Roche (Basel, Switzerland), respectively. Anti-β-Catenin (#14), anti-N-Cadherin (#32), anti-Kap3 (#14) and anti-Kif3a (#28) monoclonal antibodies were from BD Transduction (San Jose, CA, USA). Polyclonal anti-Dusp26 antibodies were described previously (Takagaki *et al.*, 2007).

*Yeast two-hybrid screening*

Full-length cDNA encoding human Dusp26 was subcloned into pBTM116-HA and used as bait to screen a human fetal brain cDNA library subcloned into pACT II (Clontech Laboratories Inc., Mountain View, CA, USA). The L40 yeast strain was transformed with bait and library plasmids, and about $3 \times 10^6$ clones were screened. A total of 22 positive clones were obtained and sequenced.

*Cell culture, transfection and retrovirus infection*

HeLa-TetOff (Clontech) and COS-7 cells were transfected using Fugene6 (Roche, Mannheim, Germany) reagent following the manufacturer's recommendation. Dusp26 expression plasmids were described previously (Takagaki *et al.*, 2007). Human Kif3a and Kap3 cDNAs were subcloned into pCMV-Myc (Clontech). For stable transfection, Flag-tagged Dusp26 cDNAs were subcloned into the retroviral vector pMXs-puro. The packaging line (PLAT-E cells; Morita *et al.*, 2000) was grown in Dulbecco's modified Eagle's medium (DMEM) with 10% fetal calf serum (FCS) and transfected with a series of pMXs-puro-Dusp26 plasmids using Fugene 6. The medium was changed the next day and further cultured for 1 day. Supernatants were used to infect NIH3T3 cells in the presence of polybrene at 7.5 μg/ml for 5 h. Infectants were selected and maintained in medium plus puromycin. Human ATC cell lines 8305C, 8505C and HTC/C3 were obtained from the Health Science Research Resources Bank (Ibaraki, Japan). 8505C and HTC/C3 cells were cultured in DMEM with 10% FCS. 8305C cells were maintained using MEM with 10% FCS. The human IMR-32 neuroblastoma line was from RIKEN Bioresource Center (Tsukuba, Japan) and cultured in MEM supplemented with nonessential amino acids (Gibco, Carlsbad, CA, USA) and 10% FCS.

*Western blot analysis*

Immunoprecipitation and western blotting were performed as described (Takagaki *et al.*, 2007). To analyse Kap3 phosphorylation, cells were washed in Hepes buffer twice, harvested and lysed in radioimmunoprecipitation assay buffer by sonication using Bio-ruptor (CosmoBio, Tokyo, Japan). Samples were separated on a 6% SDS–polyacrylamide gel, with 50 μM Phos-tag acrylamide (ALL-107) and 100 μM $MnCl_2$. Gels were soaked in transfer buffer with 5 mM EDTA for 10 min and electrotransferred.

*Immunohistochemistry*
Cells were seeded on collagen-coated coverslips in 12-well plates at $2.5 \times 10^4$ cells per well (subconfluent condition) and fixed on the next day. To obtain confluent monolayers, cells were seeded at $2 \times 10^5$ cells per well, cultured for 2 days and fixed. Immunostaining was performed as described (Takagaki *et al.*, 2007) except images were obtained using a Pascal confocal laser-scanning microscope (Zeiss, Jena, Germany). DRAQ5, a fluorescent DNA probe was obtained from Alexis (Lausen, Switzerland).

*Phosphatase assay and dephosphorylation of Kap3* in vitro
GST-Dusp26-ΔN15 was expressed in the *E. coli* DH5α strain using the pGEX system (GE Healthcare UK Ltd., Buckinghamshire, UK) and purified using glutathione sepharose 4B following the manufacturer's recommendations. pNPPase assays were performed as described previously (Takagaki *et al.*, 2007). For *in vitro* Kap3 dephosphorylation experiments, Kap3 was prepared by sonication of cells transfected with Myc-Kap3 in buffer (50 mM Tris-Cl, 150 mM NaCl, 10% glycerol, 0.1% Triton X-100). Cleared lysates were supplemented with dithiothreitol (DTT) at 5 mM and incubated with or without GST-Dusp26-ΔN15 at 30 °C for 3 h in the presence or absence of 1 mM vanadate. In Figure 4g, Myc-Kap3 was immunopurified from cells transfected Myc-Kap3 using anti-Myc-Agarose (Sigma).

*Cell aggregation assays*
Cells were trypsinized in phosphate-buffered saline supplemented with 2 mM $CaCl_2$, suspended in medium, washed with and then resuspended in medium, passed through a 27 G needle three times, and adjusted to $5 \times 10^5$ cells per ml. Cells were incubated in 1.5 ml tubes with gentle rotation at 37 °C to allow aggregate formation. After 20 min, aliquots of the suspension were evaluated and the extent of aggregation calculated by the index $(N_0–N_{20})/N_0$, where $N_{20}$ is the total particle number after 20 min incubation and $N_0$ is the total particle number at the initiation of incubation, as described previously (Ozawa *et al.*, 1990). One-way analysis of variance combined with Tukey's test was used to analyse data with unequal variance between each group. A probability level of 0.05 was considered significant.

*Primary tumor samples, qRT-PCR*
Human glioblastoma samples were obtained with informed consent from nine patients at the time of surgical removal at the Division of Neurosurgery, Miyagi Cancer Center. Histological diagnoses were based on WHO (World Health Organization) criteria by a neuropathologist. RNA analyses were approved by the institutional review of Miyagi Cancer Center. RNAs were prepared using Isogen (Nippon Gene, Tokyo, Japan) reagent and reverse-transcribed using oligo-dT primer and Superscript III RTase (Invitrogen, Carlsbad, CA, USA). Relative amounts of Dusp26 cDNA were quantified using the LightCycler 480, a LightCycler 480 probes master kit, TaqMan probe no. 79 from the universal probe library (Roche), and the Dusp26-specific primers (sense) 5′-GCTGCCGACTT CATCCAC-3′ and (antisense) 5′-CAGCACAATGCACCAG GAT-3′. Relative amounts of porphobilinogen deaminase (PBGD) mRNA was simultaneously estimated similarly using TaqMan probe no. 25 and specific primers (sense) 5′-AGCTATGAAGGATGGGCAAC-3′ and (antisense) 5′-TTGTATGCTATCTGAGCCGTCTA-3′. Human brain (frontal lobe) total RNAs from a pool of four different donors and from single donor were obtained from Clontech and BioChain Institute (Hayward, CA, USA), respectively.

**Acknowledgements**

We acknowledge Dr Konomi Kamada (Hokkaido University, Japan) for kindly providing the plasmid pBTM116-HA, the L40 yeast strain and *E. coli* HB101, and Dr Toshio Kitamura (University of Tokyo, Japan) for the pMX-puro plasmid and PLAT-E cells. Thanks are also due to E Yoshida for secretarial assistance. This work was supported in part by Grants-in-Aid for Scientific Research (B) and Grants-in-Aid for Scientific Research (C) provided by the Japan Society for the Promotion of Science of Japan.

## References

Alonso A, Sasin J, Bottini N, Friedberg I, Friedberg I, Osterman A *et al.* (2004). Protein tyrosine phosphatases in the human genome. *Cell* **117**: 699–711.

Camps M, Nichols A, Arkinstall S. (2000). Dual specificity phosphatases: a gene family for control of MAP kinase function. *FASEB J* **14**: 6–16.

Corbit KC, Shyer AE, Dowdle WE, Gaulden J, Singla V, Chen MH *et al.* (2008). Kif3a constrains beta-catenin-dependent Wnt signalling through dual ciliary and non-ciliary mechanisms. *Nat Cell Biol* **10**: 70–76.

Guillaud L, Wong R, Hirokawa N. (2008). Disruption of KIF17-Mint1 interaction by CaMKII-dependent phosphorylation: a molecular model of kinesin-cargo release. *Nat Cell Biol* **10**: 19–29.

Haraguchi K, Hayashi T, Jimbo T, Yamamoto T, Akiyama T. (2006). Role of the kinesin-2 family protein, KIF3, during mitosis. *J Biol Chem* **281**: 4094–4099.

Hirokawa N. (2000a). Determination of Left-Right Asymmetry: Role of Cilia and KIF3 Motor Proteins. *News Physiol Sci* **15**: 56.

Hirokawa N. (2000b). Stirring up development with the heterotrimeric kinesin KIF3. *Traffic* **1**: 29–34.

Hirokawa N, Tanaka Y, Okada Y, Takeda S. (2006). Nodal flow and the generation of left-right asymmetry. *Cell* **125**: 33–45.

Hu Y, Mivechi NF.. (2006). Association and regulation of heat shock transcription factor 4b with both extracellular signal-regulated kinase mitogen-activated protein kinase and dual-specificity tyrosine phosphatase DUSP26. *Mol Cell Biol* **26**: 3282–3294.

Jimbo T, Kawasaki Y, Koyama R, Sato R, Takada S, Haraguchi K *et al.* (2002). Identification of a link between the tumour suppressor APC and the kinesin superfamily. *Nat Cell Biol* **4**: 323–327.

Karcher RL, Roland JT, Zappacosta F, Huddleston MJ, Annan RS, Carr SA *et al.* (2001). Cell cycle regulation of myosin-V by calcium/calmodulin-dependent protein kinase II. *Science* **293**: 1317–1320.

Kinoshita E, Kinoshita-Kikuta E, Takiyama K, Koike T. (2006). Phosphate-binding tag, a new tool to visualize phosphorylated proteins. *Mol Cell Proteomics* **5**: 749–757.

Morita S, Kojima T, Kitamura T. (2000). Plat-E: an efficient and stable system for transient packaging of retroviruses. *Gene Ther* **7**: 1063–1066.

Nishimura T, Kato K, Yamaguchi T, Fukata Y, Ohno S, Kaibuchi K. (2004). Role of the PAR-3-KIF3 complex in the establishment of neuronal polarity. *Nat Cell Biol* **6**: 328–334.

Ozawa M, Ringwald M, Kemler R. (1990). Uvomorulin–catenin complex formation is regulated by a specific domain in the

cytoplasmic region of the cell adhesion molecule. *Proc Natl Acad Sci USA* **87**: 4246–4250.

Pulido R, Hooft van Huijsduijnen R. (2008). Protein tyrosine phosphatases: dual-specificity phosphatases in health and disease. *FEBS J* **275**: 848–866.

Takagaki K, Shima H, Tanuma N, Nomura M, Satoh T, Watanabe M *et al.* (2007). Characterization of a novel low-molecular-mass dual specificity phosphatase-4 (LDP-4) expressed in brain. *Mol Cell Biochem* **296**: 177–184.

Takeda S, Yonekawa Y, Tanaka Y, Okada Y, Nonaka S, Hirokawa N. (1999). Left-right asymmetry and kinesin superfamily protein KIF3A: new insights in determination of laterality and mesoderm induction by kif3A-/- mice analysis. *J Cell Biol* **145**: 825–836.

Teng J, Rai T, Tanaka Y, Takei Y, Nakata T, Hirasawa M *et al.* (2005). The KIF3 motor transports N-cadherin and organizes the developing neuroepithelium. *Nat Cell Biol* **7**: 474–482.

Vasudevan SA, Skoko J, Wang K, Burlingame SM, Patel PN, Lazo JS *et al.* (2005). MKP-8, a novel MAPK phosphatase that inhibits p38 kinase. *Biochem Biophys Res Commun* **330**: 511–518.

Wang JY, Lin CH, Yang CH, Tan TH, Chen YR. (2006). Biochemical and biological characterization of a neuroendocrine-associated phosphatase. *J Neurochem* **98**: 89–101.

Yu W, Imoto I, Inoue J, Onda M, Emi M, Inazawa J. (2007). A novel amplification target, DUSP26, promotes anaplastic thyroid cancer cell growth by inhibiting p38 MAPK activity. *Oncogene* **26**: 1178–1187.

Supplementary Information accompanies the paper on the Oncogene website (http://www.nature.com/onc)

Reprinted from ACTA CYTOLOGICA
Vol.53 No.1, January-February 2009



# Immunocytochemical Evaluation of Large Cell Neuroendocrine Carcinoma of the Lung

**Chiaki Endo**, M.D., **Masako Honda**, C.T., **Akira Sakurada**, M.D., **Masami Sato**, M.D., **Yasuki Saito**, M.D., and **Takashi Kondo**, M.D.

**Objective**

*To examine whether immunocytochemistry can distinguish pulmonary large cell neuroendocrine carcinoma (LCNEC) among non–small cell lung cancers (NSCLCs).*

**Study Design**

*Tumor touch imprint cytologic specimens of 109 lung cancers were studied. Immunocytochemistry was done using a total of 8 primary antibodies: chromogranin A, synaptophysin, neural cell adhesion molecule, neuron specific enolase, CK34βE12, thyroid transcription factor-1, cytokeratin 18 and E-cadherin.*

**Results**

*If 2 or 3 antibodies of chromogranin A, synaptophysin and neural cell adhesion molecule were stained positive and CK34βE12 was not stained, pulmonary LCNEC can be selected accurately among other NSCLCs with 100% sensitivity and 100% specificity.*

**Conclusion**

*This study reveals that immunocytochemistry can help distinguish LCNEC of the lung from other NSCLCs.* (Acta Cytol 2009;53:36–40)

**Keywords:** immunocytochemistry, large cell neuroendocrine carcinoma, neuroendocrine tumor, non–small cell lung cancer.

**The current study revealed that immunocytochemistry can help distinguish LCNEC accurately from other NSCLCs.**

Neuroendocrine tumors of the lung include typical carcinoid, atypical carcinoid, large cell neuroendocrine carcinoma (LCNEC) and small cell carcinoma (SCLC). Recent studies showed no prognostic difference was noted between LCNEC and SCLC.[1-3] The current World Health Organization (WHO) classification categorizes LCNEC as a variant of large cell carcinoma classified into non–small cell lung cancer (NSCLC),[4] although LCNEC is similar to SCLC from the viewpoint of the prognosis. In treatment strategy, LCNEC should be distinguished from other NSCLCs. However, the preoperative diagnosis of LCNEC is very difficult because only a small tissue specimen can be obtained preoperatively. The current study examined whether the immunocytochemistry can distinguish LCNEC from other NSCLCs.

From the Department of Thoracic Surgery, Institute of Development, Aging and Cancer, Tohoku University, Department of Thoracic Surgery, Miyagi Prefectural Cancer Center, and Department of Thoracic Surgery, Sendai Medical Center, Sendai, Japan.

Drs. Endo and Sakurada are Assistant Professors, Department of Thoracic Surgery, Institute of Development, Aging and Cancer, Tohoku University.

Ms. Honda is Cytotechnician, Department of Thoracic Surgery, Institute of Development, Aging and Cancer, Tohoku University.

Dr. Sato is Director, Department of Thoracic Surgery, Miyagi Prefectural Cancer Center.

Dr. Saito is Director, Department of Thoracic Surgery, Sendai Medical Center.

Dr. Kondo is Professor, Department of Thoracic Surgery, Institute of Development, Aging and Cancer, Tohoku University.

Address correspondence to: Chiaki Endo, M.D., Department of Thoracic Surgery, Institute of Development, Aging and Cancer, Tohoku University, 4-1 Seiryo-machi, Aoba-ku, Sendai 980-8575, Japan (endo@idac.tohoku.ac.jp).

*Financial Disclosure:* The authors have no connection to any companies or products mentioned in this article.

Received for publication December 7, 2007.

Accepted for publication December 17, 2007.



0001-5547/09/5301-0036/$21.00/0 

### *Material and Methods*

Tumor touch imprint cytologic specimens of 109 surgically resected primary lung cancers from January 2005 to April 2007 were studied. All of the cases were histologically diagnosed as primary lung cancer. The cytologic specimens were fixed with 95% ethanol; 1 was subjected to Papanicolaou staining. The others were subjected to immunocytochemistry. Primary antibodies used in the current study were mouse anti-human chromogranin A (CGA) (LK2H10, Serotec Ltd, Oxford, U.K.), rabbit anti-human synaptophysin (SYN) (Z66, Zymed Laboratories Inc, South San Francisco, California, U.S.A.), mouse anti-human neural cell adhesion molecule (NCAM) (123C3, Santa Cruz Biotechnology Inc., Santa Cruz, California, U.S.A.), mouse anti-human neuron specific enolase (NSE) (140500410, Quartett Immunodiagnostika und Biotechnologie, Berlin, Germany), mouse anti-human cytokeratins 1, 5, 10 and 14 (CK34βE12) (NCL-CK34βE12, Novocastra Laboratories Ltd, Newcastle upon Tyne, U.K.), mouse anti-human thyroid transcription factor-1 (TTF-1) (NCL-TTF-1, Novocastra), mouse anti-human cytokeratin 18 (CK18) (ab668, Abcam, Cambridge, U.K.) and mouse anti-human E-cadherin (4A2C7, Zymed). CGA, SYN, NCAM and NSE are neuroendocrine differentiation (NE) markers. CK34βE12 is a set of high molecular weight cytokeratins. TTF-1 is a 40-kDa tissue-specific homeodomain-containing transcription factor of the Nkx2 gene family that is expressed in the thyroid glands, lungs and some restricted areas of the diencephalons during development. CK18 is an acidic keratin found primarily in nonsquamous epithelia. E-cadherin is involved in the maintenance of epithelial tissue in adults.

The endogenous peroxidase activity was blocked with a 0.3% $H_2O_2$-methanol solution. After the rinse in 0.01 mol/L of phosphate-buffered saline (PBS), pH 7.4, the slides were subjected to the primary antibody reaction for 10–30 minutes. The antigen-antibody complexes were visualized using a biotin-streptavidin

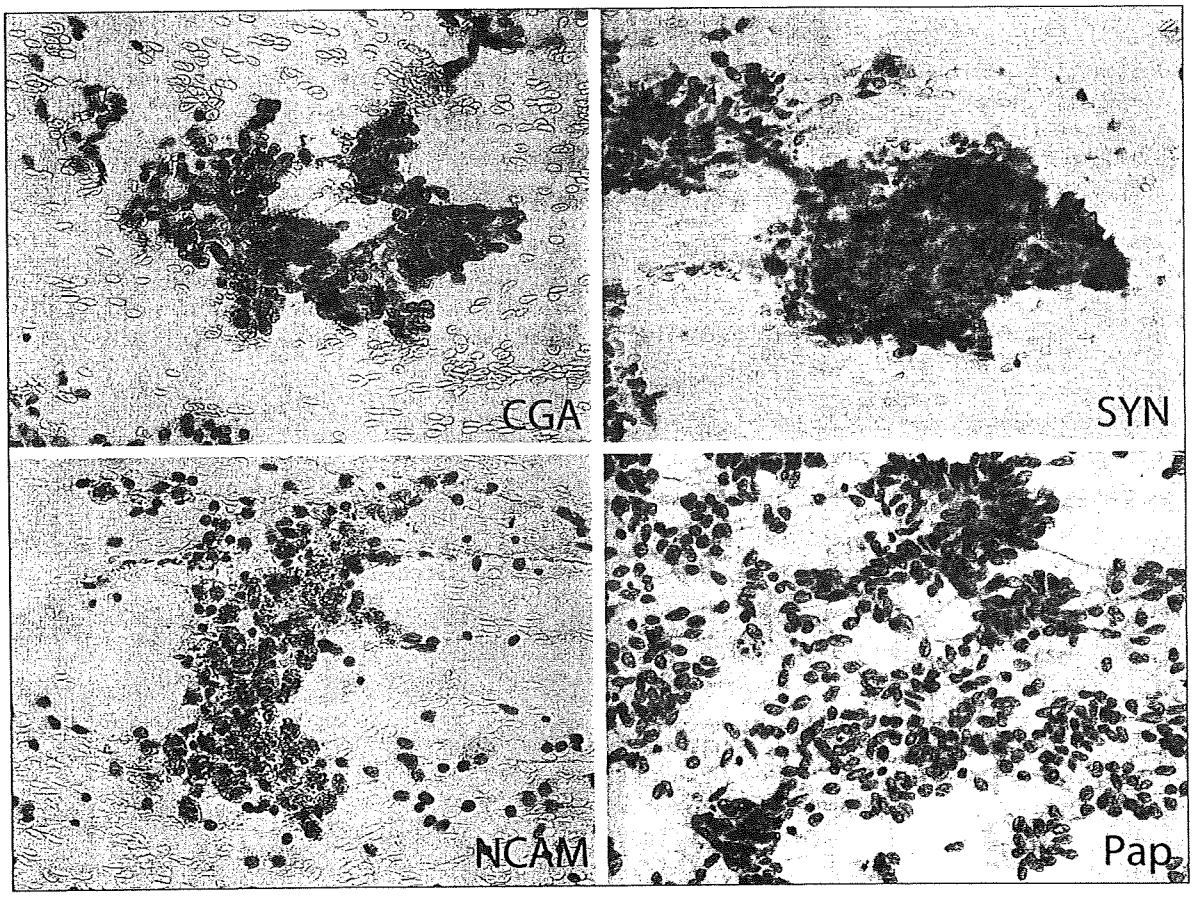


**Figure 1** Typical staining of large cell neuroendocrine carcinoma. CGA = chromogranin A, NCAM = neural cell adhesion molecule, Pap = Papanicolaou, SYN = synaptophysin (× 40).

**Table I** *Immunocytochemical Results of Various Biologic Markers*

| Tumor | CGA | SYN | NSE | NCAM | TTF-1 | CK34βE12 | CK18 | E-cadherin |
|---|---|---|---|---|---|---|---|---|
| Sq | 0/35 (0)[a] | 0/34 (0) | 7/33 (21) | 0/34 (0) | 4/35 (11) | 22/35 (63) | 17/29 (59) | 4/26 (15) |
| Ad | 2/66 (3) | 3/68 (4) | 29/67 (43) | 4/68 (6) | 45/64 (70) | 53/67 (79) | 56/63 (89) | 19/56 (34) |
| Ad with NE | 0/2 (0) | 1/2 (50) | 1/2 (50) | 1/2 (50) | 1/1 (100) | 2/2 (100) | 2/2 (100) | N/A |
| LCNEC | 2/2 (100) | 2/2 (100) | 1/2 (50) | 1/2 (50) | 0/2 (0) | 0/2 (0) | 1/1 (100) | 0/1 (0) |
| SCLC | 1/2 (50) | 0/2 (0) | 2/2 (100) | 0/2 (0) | 2/2 (100) | 1/2 (50) | 1/2 (50) | 0/2 (0) |

[a]Numbers in parentheses are percentages. Numerator is the number of positive staining and the denominator is the number of cases examined.
Fisher's exact test $p < 0.05$ Sq + Ad + Ad with NE vs. LCNEC + SCLC.
CGA and SYN stained more frequently in pulmonary neuroendocrine tumor than in non-small cell lung cancer.

detection system (Histofine immunostaining kit, Nichirei Ltd, Tokyo, Japan). In brief, the slides were incubated with biotinylated secondary antibody for 10 minutes followed by a streptavidin-peroxidase complex for 10 minutes. The peroxidase was visualized with 3-3′-diaminobenzidine tetrahydrochloride (DAB), and then the slides were counterstained lightly with hematoxylin. Immunocytochemical staining results were evaluated as negative if < 10% of tumor cells were stained or positive in the case of > 10% stained.

### Results

Histologic diagnoses of 109 cases examined were as follows; adenocarcinoma (Ad) in 68 cases, squamous cell carcinoma (Sq) in 35 cases, Ad with NE in 2 cases, LCNEC in 2 cases and SCLC in 2 cases. And these LCNEC and SCLC cases had pure histologic features, respectively. Typical positive staining was shown in Figure 1. TTF-1 was nuclear staining and the other antibodies were cytosolic staining.

The results of positive staining are shown in Table I. Some Sq and Ad showed positive staining of NSE. On the other hand, CGA and SYN stained significantly more in LCNEC and SCLC than in Sq, Ad and Ad with NE (Fisher's exact test, $p < 0.05$). TTF-1 stained more in Ad, but TTF-1 did not distinguish neuroendocrine tumor from other lung cancers because of less staining rate for Sq. CK34βE12 was stained more in nonneuroendocrine tumors, which was not statistically significant because of the insufficient number of neuroendocrine tumors. Some Sq and Ad showed positive staining of CK18 or E-cadherin, so these 2 antibodies were not useful for differential diagnosis of LCNEC.

Table II shows the positive staining rate of NE marker for Ad and Sq stratified with tumor differentiation. Tumor differentiation of Ad and Sq was not correlated to the NE marker staining rate.

CGA, SYN and NCAM were selected to examine whether a combination of these 3 markers was useful to distinguish neuroendocrine tumor from other lung cancers, because NSE was stained in some cases of Ad and Sq. Table III shows the positive staining rate of multiple neuroendocrine markers. Of 66 adenocarcinomas, 4 (6%) showed positive staining of any 1 of 3 NE markers. Only 1 adenocarcinoma showed positive staining of any 2 markers.

From the results stated above, CGA, SYN, NCAM and CK34βE12 were selected to examine whether these 4 antibodies can distinguish LCNEC from other NSCLCs. If 2 or 3 antibodies of CGA, SYN and NCAM were stained positive and CK34βE12 was not stained, LCNEC can be selected accurately among other NSCLCs with 100% sensitivity and 100% specificity (Table IV).

### Discussion

LCNEC was first described in 1991.[5] In the WHO

**Table II** *Immunocytochemical Results of Various Biologic Markers Stratified with Histology Type and Tumor Differentiation*

| | CGA | SYN | NSE | NCAM | TTF-1 | CK34βE12 | CK18 | E-cadherin |
|---|---|---|---|---|---|---|---|---|
| Adenocarcinoma | | | | | | | | |
| Well | 1/27 (4)[a] | 1/29 (3) | 10/28 (36) | 2/29 (7) | 20/28 (71) | 22/29 (76) | 23/26 (88) | 7/23 (30) |
| Moderate | 1/22 (5) | 1/22 (5) | 14/22 (64) | 2/22 (9) | 16/20 (80) | 15/21 (71) | 18/20 (90) | 7/18 (39) |
| Poor | 0/17 (0) | 1/17 (6) | 5/17 (29) | 0/17 (0) | 9/16 (56) | 16/17 (94) | 15/17 (88) | 5/16 (31) |
| Squamous cell carcinoma | | | | | | | | |
| Well | 0/7 (0) | 0/7 (0) | 2/7 (29) | 0/7 (0) | 1/7 (14) | 3/7 (43) | 1/4 (25) | 1/4 (25) |
| Moderate | 0/23 (0) | 0/22 (0) | 4/21 (19) | 0/22 (0) | 2/23 (9) | 15/23 (65) | 12/20 (60) | 1/17 (6) |
| Poor | 0/5 (0) | 0/5 (0) | 1/5 (20) | 0/5 (0) | 1/5 (20) | 4/5 (80) | 4/5 (80) | 2/5 (10) |

[a]Numbers in parentheses are percentages. Numerator is the number of positive staining and the denominator is the number of cases examined.
Positivity rate of antibodies examined was not correlated with tumor differentiation of both adenocarcinoma and squamous cell carcinoma.

**Table III** *Immunocytochemical Results of Neuroendocrine Markers*

| Tumor | Any 1 of CGA, SYN and NCAM | Any 2 of CGA, SYN and NCAM | Any 3 of CGA, SYN and NCAM |
|---|---|---|---|
| Sq | 0/34 (0)[a] | 0/34 (0) | 0/34 (0) |
| Ad | 4/66 (6) | 1/66 (2) | 0/66 (0) |
| Ad with NE | 1/2 (50) | 1/2 (50) | 0/2 (0) |
| LCNEC | 0/2 (0) | 1/2 (50) | 1/2 (50) |
| SCLC | 0/2 (0) | 1/2 (0) | 0/2 (0) |

[a]Numbers in parentheses are percentages. Numerator is the number of positive staining and the denominator is the number of cases examined.
Four of 66 Ads (6%) showed positive staining of any 1 of 3 NE markers. Only 1 adenocarcinoma showed positive staining of any 2 markers.

revised classification in 1999, LCNEC was classified as a variant of large cell carcinoma and also categorized in neuroendocrine tumors of the lung.[4] The major categories of neuroendocrine tumors are SCLC, LCNEC, atypical carcinoid and typical carcinoid. The major focus of differential diagnosis of LCNEC has so far been to distinguish it from SCLC.[6-8] However, it has been sometimes difficult preoperatively to distinguish LCNEC from other NSCLCs such as classic large cell carcinoma, poorly differentiated Ad or poorly differentiated Sq even after the WHO revised classification became well known. Doddoli et al[9] reported clinicopathologic characteristics of 20 cases of LCNEC who underwent anatomic resection. Eleven cases had a preoperative diagnosis of lung cancer. Among them, 4 had a preoperative diagnosis of LCNEC and 7 cases had a diagnosis of undifferentiated NSCLC. As a result, among LCNEC cases who had a preoperative diagnosis of lung cancer, ~64% (7 of 11) were diagnosed as having NSCLC except LCNEC. Paci et al[10] reported 48 patients with surgically resected LCNEC. A preoperative diagnosis of LCNEC was not made for any of the cases, and 27 cases had a preoperative diagnosis of NSCLC, which meant all patients who had a preoperative diagnosis were diagnosed as NSCLC except LCNEC.

Because only a small tissue specimen can be obtained preoperatively, it is quite difficult to diagnose histologically even if immunohistochemistry (IHC) can be done. On the other hand, a sufficient quantity of cytologic specimens to be diagnosed can be relatively easily obtained by bronchoscopy, percutaneous needle aspiration and so on. Accordingly, cytologic evaluation may be useful and helpful to the preoperative diagnosis. However, cytomorphologic approach with Papanicolaou staining has shown difficulty in distinguishing accurately between LCNEC and SCLC.[8] Therefore, in the present study, immunocytochemistry was used in addition to the usual morphologic approach with Papanicolaou staining.

The current study revealed that immunocytochemistry can help distinguish LCNEC accurately from other NSCLCs. Our results indicated that 5 slides (Papanicolaou, CGA, NCAM, SYN and 34βE12) could be enough to diagnose cytologically in each case.

Poorly differentiated Ad or Sq is sometimes difficult to distinguish morphologically from LCNEC. However, tumor differentiation of Ad and Sq was not correlated to the staining rate of CGA, SYN, NCAM and CK34βE12. Thus our criteria can distinguish LCNEC even from poorly differentiated NSCLC.

The drawback of the present study is the insufficient number of LCNEC cases examined. The reasonable question that the present study cannot answer precisely is how frequently LCNEC is stained with CK34βE12 or NE markers. Consider the following published reports. Peng et al[6] examined 16 cases of LCNEC and 9 cases of large cell carcinoma with neuroendocrine morphology (LCCNM) with IHC. They reported that CK34βE12 produced negative results in 14 cases of LCNEC (88%) and positive results in 6 cases of LCCNM (67%). They also reported CGA had the highest specificity among NE markers. Harada et al[11] studied immunohistologically 13 cases of LCNEC and reported all cases had positive staining for either CGA or SYN. Sturm et al[12] reported CK34βE12 expression of 64 cases of LCNEC, 56 cases of SCLC and 50 cases of carcinoids. All of these

**Table IV** *Immunocytochemical Results of CGA, SYN, NCAM and CK34βE12*

| | 2 or 3 positive staining among CGA, SYN and NCAM, and negative staining of CK34βE12 |
|---|---|
| Sq | 0/34 |
| Ad | 0/66 |
| Ad with NE | 0/2 |
| LCNEC | 2/2 |
| SCLC | 0/2 |

The denominator means the number of cases examined, and the numerator means the number of cases showing any 2 or all positive staining among CGA, SYN and NCAM, and negative staining of CK34βE12.
If 2 or 3 markers of CGA, SYN and NCAM were stained positive and CK34βE12 was not stained, LCNEC can be selected accurately among other NSCLCs with 100% sensitivity and 100% specificity.

NE tumors were consistently negative staining, suggesting CK34βE12 expression excludes the NE tumors of the lung. All of these immunohistochemical studies support our results and proposal.

TTF-1 was also evaluated in the current study. Sturm et al[13] reported that positive immunostaining for TTF-1 was detected in 49% of LCNECs. Zamecnik and Kodet[14] showed that positive staining for TTF-1 was found in 75% of Ad, 50% of pure large cell carcinomas and none of Sq. These reports and our results suggested that CK34βE12 was more helpful than TTF-1 in distinguishing between other NSCLCs and LCNECs.

Nitadori et al[7] showed that expression of CK18 and E-cadherin was more characteristic of LCNEC than of SCLC. However, our results indicated CK18 and E-cadherin were not useful in distinguishing between LCNEC and other NSCLCs.

Marmor et al[15] reported transthoracic fine needle aspiration (FNA) in the diagnosis of LCNEC. Cytologic materials were immunostained with NSE, CGA and SYN. Because they did not examine NSCLC, except LCNEC, the accuracy of their procedure to distinguish LCNEC from other NSCLCs was not known. But they showed transthoracic FNA can be used for the immunostaining of cytologic materials. We used tumor touch imprint as a cytologic specimen in the current examination. Our procedure was completed in an hour; thus it can be easily applied in cytologic diagnosis during surgical operation. We plan to use transthoracic FNA for preoperative diagnosis, using 5 smear slides—Papanicolaou, CGA, SYN, NCAM and 34βE12—for preoperative diagnosis of LCNEC.

### *References*


1. Asamura H, Kameya T, Matsuno Y, Noguchi M, Tada H, Ishikawa Y, Yokose T, Jiang SX, Inoue T, Nakagawa K, Tajima K, Nagai K: Neuroendocrine neoplasms of the lung: A prognostic spectrum. J Clin Oncol 2006;24:70–76
2. Iyoda A, Hiroshima K, Nakatani Y, Fujisawa T: Pulmonary large cell neuroendocrine carcinoma: Its place in the spectrum of pulmonary carcinoma. Ann Thorac Surg 2007;84:702–707
3. Yamazaki S, Sekine I, Matsuno Y, Takei H, Yamamoto N, Kunitoh H, Ohe Y, Tamura T, Kodama T, Asamura H, Tsuchiya R, Saijo N: Clinical responses of large cell neuroendocrine carcinoma of the lung to cisplatin-based chemotherapy. Lung Cancer 2005;49:217–223
4. Brambilla E, Travis WD, Colby TV, Corrin B, Shimosato Y: The new World Health Organization classification of lung tumours. Eur Respir J 2001;18:1059–1068
5. Travis WD, Linnoila RI, Tsokos MG, Hitchcock CL, Cutler GB Jr, Nieman L, Chrousos G, Pass H, Doppman J: Neuroendocrine tumors of the lung with proposed criteria for large-cell neuroendocrine carcinoma: An ultrastructural, immunohistochemical, and flow cytometric study of 35 cases. Am J Surg Pathol 1991;15:529–553
6. Peng WX, Sano T, Oyama T, Kawashima O, Nakajima T: Large cell neuroendocrine carcinoma of the lung: A comparison with large cell carcinoma with neuroendocrine morphology and small cell carcinoma. Lung Cancer 2005;47:225–233
7. Nitadori J, Ishii G, Tsuta K, Yokose T, Murata Y, Kodama T, Nagai K, Kato H, Ochiai A: Immunohistochemical differential diagnosis between large cell neuroendocrine carcinoma and small cell carcinoma by tissue microarray analysis with a large antibody panel. Am J Clin Pathol 2006;125:682–692
8. Hiroshima K, Abe S, Ebihara Y, Ogura S, Kikui M, Kodama T, Komatsu H, Saito Y, Sagawa M, Sato M, Tagawa Y, Nakamura S, Nakayama T, Baba M, Hanzawa S, Hirano T, Horai T: Cytological characteristics of pulmonary large cell neuroendocrine carcinoma. Lung Cancer 2005;48:331–337
9. Doddoli C, Barlesi F, Chetaille B, Garbe L, Thomas P, Giudicelli R, Fuentes P: Large cell neuroendocrine carcinoma of the lung: An aggressive disease potentially treatable with surgery. Ann Thorac Surg 2004;77:1168–1172
10. Paci M, Cavazza A, Annessi V, Putrino I, Ferrari G, De Franco S, Sgarbi G: Large cell neuroendocrine carcinoma of the lung: A 10-year clinicopathologic retrospective study. Ann Thorac Surg 2004;77:1163–1167
11. Harada M, Yokose T, Yoshida J, Nishiwaki Y, Nagai K: Immunohistochemical neuroendocrine differentiation is an independent prognostic factor in surgically resected large cell carcinoma of the lung. Lung Cancer 2002;38:177–184
12. Sturm N, Rossi G, Lantuejoul S, Laverriere MH, Papotti M, Brichon PY, Brambilla C, Brambilla E: 34BetaE12 expression along the whole spectrum of neuroendocrine proliferations of the lung, from neuroendocrine cell hyperplasia to small cell carcinoma. Histopathology 2003;42:156–166
13. Sturm N, Rossi G, Lantuejoul S, Papotti M, Frachon S, Claraz C, Brichon PY, Brambilla C, Brambilla E: Expression of thyroid transcription factor-1 in the spectrum of neuroendocrine cell lung proliferations with special interest in carcinoids. Hum Pathol 2002;33:175–182
14. Zamecnik J, Kodet R: Value of thyroid transcription factor-1 and surfactant apoprotein A in the differential diagnosis of pulmonary carcinomas: A study of 109 cases. Virchows Arch 2002; 440:353–361
15. Marmor S, Koren R, Halpern M, Herbert M, Rath-Wolfson L: Transthoracic needle biopsy in the diagnosis of large-cell neuroendocrine carcinoma of the lung. Diagn Cytopathol 2005;33: 238–243